

## Crystallographic Orientation and Deformation Mechanisms of Laser-processed Directionally Solidified WC-W<sub>2</sub>C Eutectoids

Wei-Ting Chen<sup>1</sup> and Elizabeth C. Dickey<sup>1</sup>

<sup>1</sup>Department of Materials Science and Engineering, North Carolina State University, Raleigh, NC, USA

Ceramic composites with excellent mechanical performance have been used in applications such as cutting tools and ceramic drilling bits for many decades. Carbides are the most prevalent materials in these applications due to their high hardness, melting temperature, and wear resistance. However, most monolithic carbides suffer from low sinterability and low fracture toughness. WC-Co composites have been widely used for improving densification of WC while also improving fracture toughness, although the addition of the metal content sacrifices hardness, oxidation resistance, and thermal stability [1]. Directionally solidified WC-W<sub>2</sub>C eutectoids (WC-W<sub>2</sub>C DSE) at the eutectoid composition are being explored as an alternative composite structure that may provide a path for highly dense materials with high hardness without sacrificing oxidation resistance and thermal stability. WC-W<sub>2</sub>C DSEs at 40 at % carbon were produced at laser processing rates between 0.12-3.24 mm/s and a laser power of 2000 W. The relationship between laser processing rate ( $V$ ) and interlamellar spacing ( $\lambda$ ) follows the equation:  $V\lambda^{3.8} = constant$ , typical of a eutectoid transformation. The indentation hardness was found to increase with decreasing interlamellar spacing via a power-law relationship with an exponent of -2.4, with a maximum hardness of  $28.2 \pm 0.33$  GPa measured at an interlamellar spacing of  $331 \pm 36$  nm. This value is 28% higher than the highest hardness (22 GPa) measured in WC-Co composites (12 wt % Co) [2].

The present work aims to study microstructure, crystallography and deformation mechanisms in laser-processed WC-W<sub>2</sub>C DSE, to understand the role of the microstructure on the hardness scaling. Microstructure and crystallographic orientation relationships of WC-W<sub>2</sub>C composites are investigated by electron backscattered diffraction (EBSD) in a scanning electron microscope. As shown in Fig. 1(a), a lamellar-typed microstructure is observed in all samples. As evident in Fig. 1(b), the majority of the material has the orientations of WC[ $\bar{1}2\bar{1}0$ ]/W<sub>2</sub>C[ $\bar{1}2\bar{1}0$ ] or WC[01 $\bar{1}0$ ]/W<sub>2</sub>C [01 $\bar{1}0$ ] parallel to the growth direction. In Fig. 1(c), the preferred in-plane orientation was found to be WC(0001)/W<sub>2</sub>C(0001), while higher misorientations may be due to the precipitation of the primary WC prior to the eutectoid reaction [3]. STEM images (Fig. 2) indicate that the interface plane is faceted parallel to WC(0001)/W<sub>2</sub>C(0001), and that it is semi-coherent, with the Burger's circuit indicating the presences of one misfit dislocation every 39 d(01 $\bar{1}0$ ) WC to accommodate the 2.6% lattice mismatch.

Deformation mechanisms induced by indentation are studied by using bright-field TEM imaging under several two-beam conditions. As shown in Fig. 3(a)(b), although dislocations are observed in the as-processed sample, shear banding and grain refinement are the dominant deformation mechanisms in W<sub>2</sub>C-rich regions. As shown in Fig. 4(a), dislocation networks with Burger's vector parallel to  $\langle 11\bar{2}0 \rangle$  bounding stacking faults with displacement vectors parallel to  $\langle \bar{2}1\bar{1}\bar{3} \rangle$  are commonly observed in the primary WC phase. The regions containing eutectoid (fine lamellae) microstructure exhibit markedly different deformation mechanisms. Shear banding is suppressed in W<sub>2</sub>C lamellae. Moreover, as shown in Fig. 4(b), partial dislocations with the Burger's vector along  $\langle 1\bar{2}13 \rangle$  are observed within the WC lamellae, and these dislocations and stacking faults are interrupted at the interfaces, which implies that interface density and corresponding microstructural length scale may have significant impacts on hardness of WC-W<sub>2</sub>C DSE [4].

References:

- [1] Lee, H.C. *et al*, *J. Mater. Sci. and Eng.*, **33** (1978), p. 125-133.
- [2] Michalski, A. *et al*, *Int. J. Refract. Met. & Hard Mater.*, **25** (2007), p. 153-158.
- [3] Kurlov, A.S. *et al*, *Inorg. Mater.*, **42** (2006), p. 121-127.
- [4] The authors acknowledge funding from National Science Foundation (Grant # CMMI-1139792).

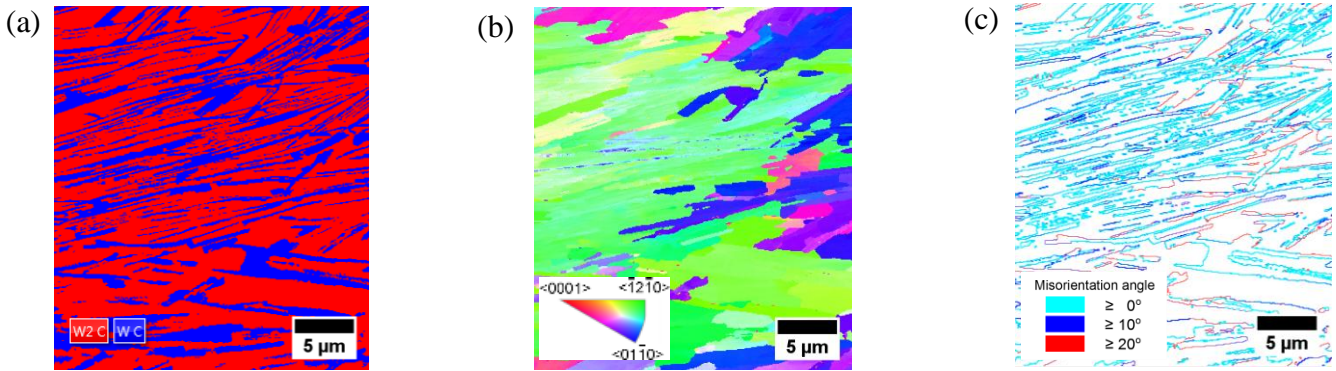


Figure 1 – EBSD (a) phase map (b) orientation map ( $\parallel$  growth direction) (c) WC(0001)/W<sub>2</sub>C(0001) interface orientation map of DSE WC-W<sub>2</sub>C produced at 0.12 mm/s processing rate.

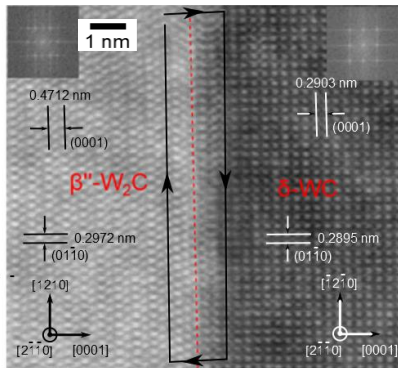


Figure 2 – STEM image of the WC(0001)/W<sub>2</sub>C(0001) interface.

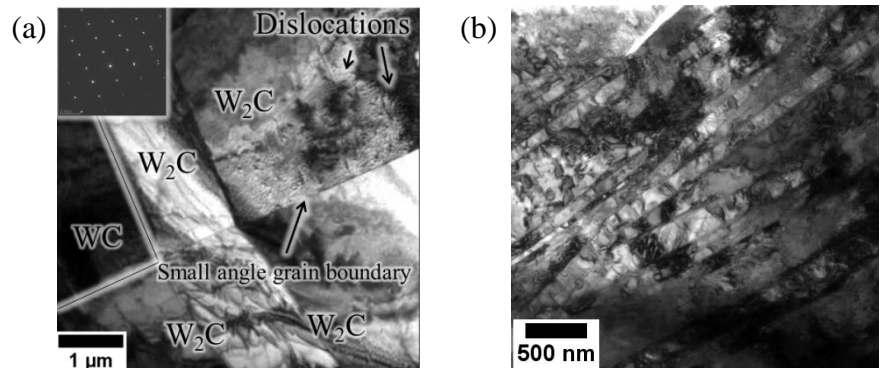


Figure 3 – TEM images of (a) undeformed (b) deformed W<sub>2</sub>C-rich region. Samples were produced at 0.12 mm/s processing rate

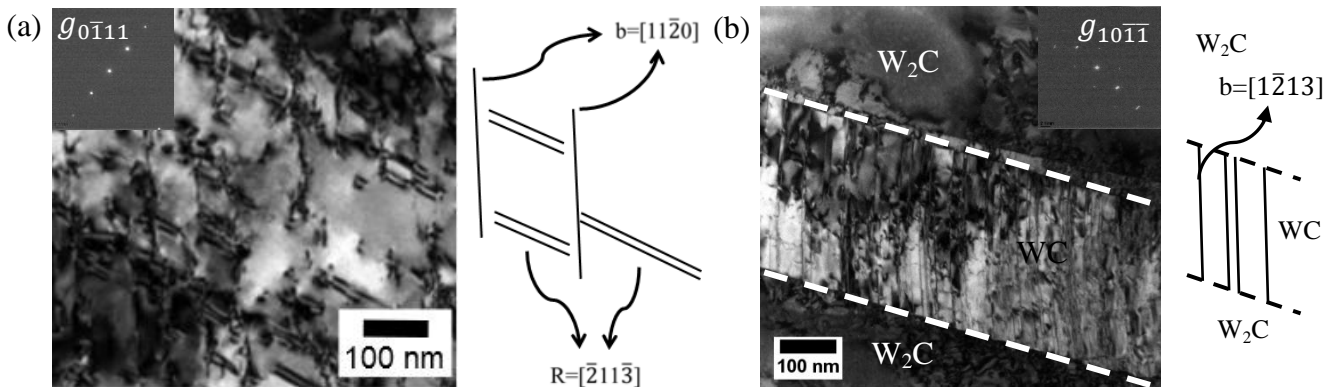


Figure 4 – TEM bright field images of the indentation-induced deformed samples by 4.9 N load produced at 0.12 mm/s processing rate in (a) primary WC region and (b) WC lamellae region. The indexing of the dislocations is showed at the right side of each image.